# Fatigue crack initiation and growth in a CrMo steel under hydrogen pressure

Laurent Briottet, Isabelle Moro, Marielle Escot, Jader Furtado, Paolo Bortot, Gian Marco Tamponi, Jouni Solin, Grégory Odemer, Christine Blanc, Eric Andrieu

# Fatigue crack initiation and growth in a CrMo steel under hydrogen pressure

L. Briottet [a,b,*], I. Moro [a,b], M. Escot [a,b], J. Furtado [c], P. Bortot [d], G.M. Tamponi [e], J. Solin [f], G. Odemer [g], C. Blanc [g], E. Andrieu [g]

[a] Univ. Grenoble Alpes, F-38000 Grenoble, France
[b] CEA, LITEN, DTBH, F-38054 Grenoble, France
[c] Air Liquide — Centre de Recherche Paris-Saclay, 1 chemin de la Porte des Loges, BP 126, 78354 Les Loges-en-Josas, Jouy-en-Josas, France
[d] TenarisDalmine R&D, Piazza Caduti 6 Luglio 1944, 1, 24044 Dalmine, Italy
[e] CSM SPA, Via Di Castel Romano 100, Roma 00128, Italy
[f] VTT Technical Research Centre of Finland, Vuorimiehentie 5, Espoo 02044, Finland
[g] Université de Toulouse, CIRIMAT, UPS/INPT/CNRS, ENSIACET, 4 allée Emile Monso, BP 44362, 31030 Toulouse Cedex 4, France

## A B S T R A C T

*Keywords:*
Pressure vessel
Hydrogen embrittlement
Design codes
Fatigue crack initiation
Fatigue crack growth

Along the hydrogen supply chain, metallic components, such as pressure vessels, compressors and valves, are facing high pressure hydrogen gas. The object of this paper is to address microstructural as well as mechanical aspects of fatigue crack initiation and growth at room temperature in a quenched and tempered (Q&T) low alloy steel under hydrogen pressure in the range 0.5—35 MPa. For such steel, the need to perform tests in-situ under hydrogen pressure is required. The influence of hydrogen gas on the total life in terms of crack initiation and crack propagation is analyzed. The experimental techniques developed to detect crack initiation in a pressure vessel under hydrogen pressure are presented. Thanks to these technical developments the influence of hydrogen gas on the total life duration including crack initiation and crack propagation is analyzed. It is shown that the effect of hydrogen pressure on crack initiation is important. At constant load ratio, the hydrogen pressure effect on fatigue crack growth (FCG) is dependent on the loading amplitude (in terms of ΔK). These results related to cracking behavior are enriched with information on fracture surfaces appearance. The results presented have been achieved within the European project MATHRYCE [1] dedicated to Material Testing and Recommendations for Hydrogen Components under fatigue. They are part of a process necessary to give a scientific background to the development of a design methodology where hydrogen enhanced fatigue damage is taken into account.

## Introduction

Pressure vessels for gaseous hydrogen storage can be submitted to several pressure cycles, therefore taking hydrogen enhanced fatigue damage into account is a key step for a safe design and a large development of hydrogen economy. Several works are currently performed on this subject [1–3]. The European MATHRYCE project aims to propose an easy way to implement vessel design methodology based on lab-scale tests taking into account hydrogen enhanced fatigue damage [1]. Due to the components considered in this study and their associated estimated maximum number of cycles in use, low cycle fatigue (LCF) loading is involved when a defect or a crack is present. Many studies have shown that the fatigue life of LCF samples is strongly reduced when tested under hydrogen pressure. The effect of hydrogen on fatigue crack growth has been intensively addressed. The fatigue crack growth rate of Cr–Mo steels is classically observed to be enhanced by a factor 20–30 at sufficiently high ΔK. By contrast, the effect of hydrogen on fatigue crack initiation (FCI) under LCF conditions has not widely been studied since it is believed that for such loading, FCI is not predominant [4]. However, considering a strong decrease of fatigue life time under hydrogen due to accelerated FCG, the life spent in fatigue crack initiation may become important.

The present paper focuses on a low alloy Q&T Cr–Mo steel, classically used to store hydrogen gas up to 45 MPa. Hydrogen enhanced fatigue has been addressed in terms of crack initiation and propagation, in particular to clarify the respective contribution of these two stages of the fracture process with or without hydrogen, analyzing the possible effects of the gas pressure, load-cycle frequency, minimum load/maximum load ratio R. The developed methodology to detect crack initiation under hydrogen pressure is described and validated. Then, the fatigue crack behavior is discussed together with fracture surface observations.

## Material and methods

### Material

The material used in this study is a 25CrMo4 steel according to EN 10083-3 standard (Table 1). Specimen were machined from a commercially available seamless pressure vessel OD 470 mm x WT 30 mm (Fig. 1). The mechanical properties of this material in the transverse direction are 630 MPa for the yield stress and 785 MPa for the ultimate tensile strength, whereas the total elongation is 19%.

| Table 1 – Chemical composition (wt %) of the product under investigation. | | | | | |
|---|---|---|---|---|---|
| | C | Si | Mn | Cr | Mo |
| Standard requirements | 0.22–0.29 | Max 0.4 | 0.6–0.9 | 0.9–1.2 | 0.15–0.30 |
| Product analysis | 0.26 | 0.24 | 0.76 | 0.98 | 0.20 |

The material is provided in a Q&T state. Microstructure (Fig. 1) has been analysed by means of Electron Back Scattered Diffraction (EBSD) technique. In particular, packets, which are the regions separated by high-angle (>15°) boundaries, were identified through Inverse Pole Figure (IPF) maps obtained by EBSD at mid-wall. Coarse packets were related to tempered bainite, whereas fine packets are likely associated with regions constituted of tempered martensite. The size of the prior austenitic grans has been evaluated around 30–50 μm using EBSD and the ARPGE software [15] to reconstruct the parent grains (Fig. 2).

As small differences in composition, microstructure or non-metallic inclusions can be important when dealing with fatigue resistance under hydrogen environment, a detailed microstructural analysis has thus been performed on the components selected for the project. The observed inclusions are mainly constituted by fine globular sulfides and oxides and by sporadic aluminates. The analysis of these non-metallic inclusions was also done, investigating both the maximum dimension and shape of the inclusions typical for the product. Two methods have been used: the Automatic Inclusion Analysis and the Analysis of Non Metallic Inclusions according to ESIS/ASTM standards (Linear Extreme Value Distribution) [5,6].The resulting maximum expected inclusion size for the component was predicted to be 120 μm, as per the extreme value analysis. This is based on the largest dimension of the inclusions as observed in metallographic survey. The largest expected non-metallic inclusion is sensibly smaller than detection limits, with adequate probability of detection, of non-destructive examination (NDE) techniques commonly used for industrial structural elements. As an example ISO 11120–1999 [7] prescribes an ultrasonic inspection given where the reference notch depth is set to 5% of the nominal wall thickness with a maximum depth of 1 mm. For conservativeness purposes, the minimum defect dimension to be considered in the following of the study will be based on this NDE limit.

### General testing procedure

All the tests were performed at room temperature (RT) on an MTS servo-hydraulic testing system in a pressure vessel filled with gaseous hydrogen up to 35 MPa. The quality of the hydrogen gas was a 6.0 high purity. In order to ensure a good and reproducible environment quality, a specific procedure, including several vacuum plus 6.0 nitrogen filling runs was followed. A final filling of the vessel with 6.0 pure nitrogen is performed at the testing pressure. Finally, hydrogen is introduced and a 30 min dwell at the $H_2$ testing pressure was performed before carrying out the mechanical tests under hydrogen. This experimental procedure ensures a reproducible testing atmosphere and a low level of $H_2O$ and $O_2$ impurity contents, below a few ppm. Indeed, it is recognized that a higher level of impurity may have an impact on the hydrogen embrittlement sensitivity of metallic materials [23].

### Fatigue crack initiation

The classical effect of hydrogen on steels is to reduce their fatigue life. In particular, it is well known that fatigue crack
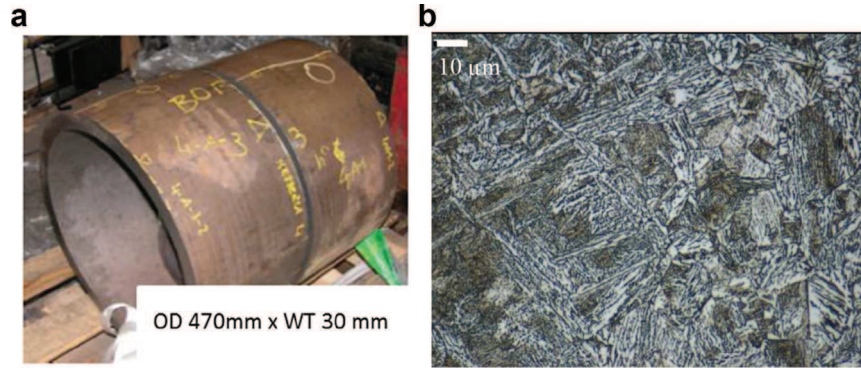
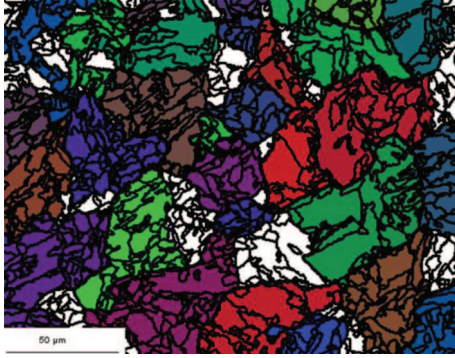**Fig. 1 – (a) 25CrMo4 steel jumbo and (b) microstructure of mixed Tempered bainite-martensite.**



**Fig. 2 – Example of reconstruction of austenitic parent grains with the ARPGE software (using the Greninger-Troiano orientation relationship) [15].**

growth is accelerated under hydrogen pressure. Therefore, crack initiation stage might play a role with respect to the total life duration of a component submitted to hydrogen gas (Fig. 3). In other words, it is important to know whether the respective parts of these two processes are affected by the presence of hydrogen pressure or not (equation (1)).

$$\left(\frac{N_{init}}{N_{propag}}\right)_{air} \overset{?}{\ll} \left(\frac{N_{init}}{N_{propag}}\right)_{H_2} \tag{1}$$
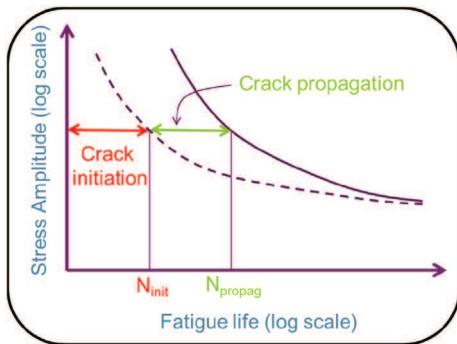


**Fig. 3 – Relative crack initiation and propagation part on the total fatigue life.**

Fatigue crack initiation under low cycle fatigue conditions occurs on (or near) the surface of the specimens. Addressing crack initiation under hydrogen gas raises the question of the most appropriate sample geometry, in particular if smooth or notched specimens have to be used. In the latter case, it is difficult to define which notch geometry should be considered. The preferential sites of crack initiation are surface roughness, geometrical stress concentrators, coarse grains, large non-metallic inclusions and persistent slip bands [8]. Thus, crack initiation occurs randomly on the surface of the specimen, which complicates the method to detect this phenomenon.

To overcome this problem, crack initiation may be studied using a specimen containing a hole or a notch. The presence of a defect (hole, notch) on specimen increases the stress-concentration and modifies the hydrostatic stress in the process zone ahead of the defect, influencing locally the hydrogen content [9,10]. It also changes the local loading. Indeed, in presence of a defect, a remote cyclic tension–tension load control loading shifts locally to a tension-compression strain control (Fig. 4). Moreover, when a small crack initiates from this defect, its initial growth is affected by the strain field induced by the defect. Whereas after some propagation, the crack will behave independently (Fig. 4). Thus, the specimen geometry and testing conditions have to be reported carefully when comparing these types of tests. The results concerning the number of cycles for crack initiation are very dependent on the fatigue testing conditions, material and hydrogen pressure.
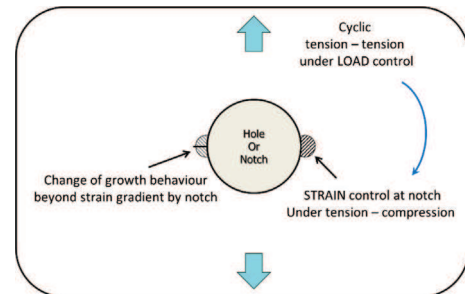


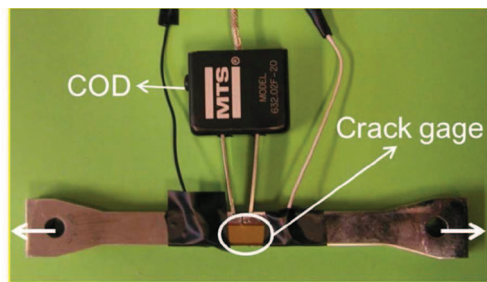**Fig. 4 – Several local notch mechanical effects.**

**Fig. 5 – SENT specimen with a crack gage and a clip gage.**

Murakami [8] developed a methodology based on cylindrical specimens with a calibrated hole for fatigue tests to study both crack initiation and propagation. This methodology has been applied to address hydrogen embrittlement on hydrogen pre-charged specimens [11]. The fatigue crack length is recorded using the replica method during the fatigue test to study crack propagation. In this method, the diameter of the hole is representative of the size of the largest non-metallic inclusion using the extreme value analysis [5,6,8]. However, due to the high hydrogen diffusivity in ferritic low alloy steels, tests on hydrogen precharged specimen may not be representative of the behavior of the steels working under hydrogen gas. Thus, as the fatigue tests have to be performed in-situ under hydrogen pressure, this method, based on replicas, cannot be applied inside the testing chamber.

When dealing with crack initiation, it is necessary to define a quantitative value that clearly identifies the onset of crack initiation. Although several arguments may be discussed, in the present study, crack initiation is defined as the smallest crack that can be detected under the testing conditions constrained by the presence of a pressure vessel and hydrogen gas.

Considering the above observations, as well as safety issues, crack gages on SENT specimen were chosen (Fig. 5). The radius of the notch was set to 0.2 mm. It has been defined from Finite Element simulations in order to reproduce stress-strain fields similar to that found in front of an artificial notch machined in a pressure vessel to be tested under cyclic hydrogen pressure [12]. Moreover, the SENT geometry, instead of a CT geometry, was chosen to have a crack propagation in the same direction as the expected one of a crack in the full scale gas cylinder.

Within the Mathryce project, artificial notches on the internal surfaces of full scale cylinders have also been introduced for comparison with lab-scale further predictions. In order to have the same type of notches in both geometries (local microstructure in front of the notch), the notches were also machined by electro discharge machining (EDM) in the SENT specimen.

Strain gages used under hydrogen pressure usually present a shift of their signal that may or may not saturate in a reasonable time, due to hydrogen permeation in the glue, the substrate and/or the metallic parts. The use of crack gages avoid this problem as shown in Fig. 6 corresponding to a test performed at 10 MPa H$_2$. Each time a copper wire is broken by the crack propagation, a clear potential drop is observed. Each crack gage consists of 50 copper wires, 50 μm thick, spaced by 50 μm of electrical insulator [13]. Using this crack gage, with a special procedure to stick it on the notch tip, crack initiation corresponds to a crack length less than 100 μm.

For these tests, due to experimental constraints, only one crack gage on one side of the sample was used. The optical analysis of the specimen tested under air gives an idea of the uniformity of crack initiation. A maximum factor of 2 in the number of cycles to create a 0.1 mm surface crack could be observed between both sides of a given specimen. Interrupted tests under hydrogen pressure confirmed this ratio. This disparity can be caused by the fact that micro-cracks initiate first independently along the 10 mm large notch before forming a single crack across the whole specimen. A second cause could be the testing device misalignment. However, the alignment was considered acceptable since the crack front obtained after a few mm growth was reasonably parallel to the notch front.

*Fatigue crack growth*

SENT and CT specimens were used to address fatigue crack growth under hydrogen pressure in the same testing device as described above. Fatigue crack growth has been measured by two different techniques. First with the compliance method using an MTS crack opening displacement (COD) device as shown in Fig. 5. Second, the crack gage can also be used to this
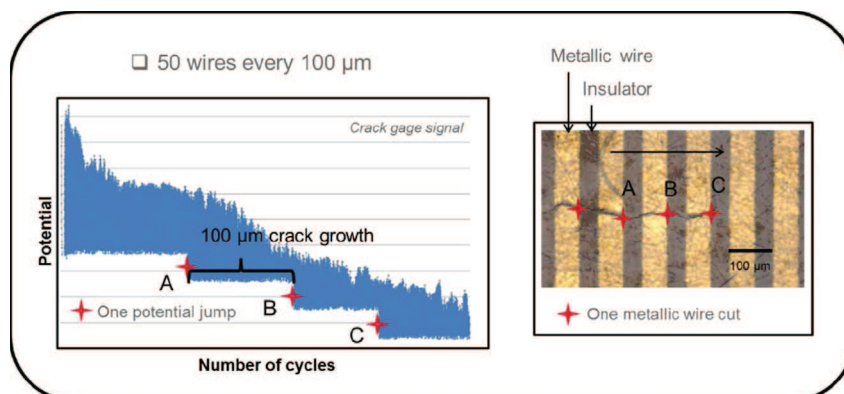


**Fig. 6 – Validation of the crack gage output signal under 10 MPa H$_2$.**
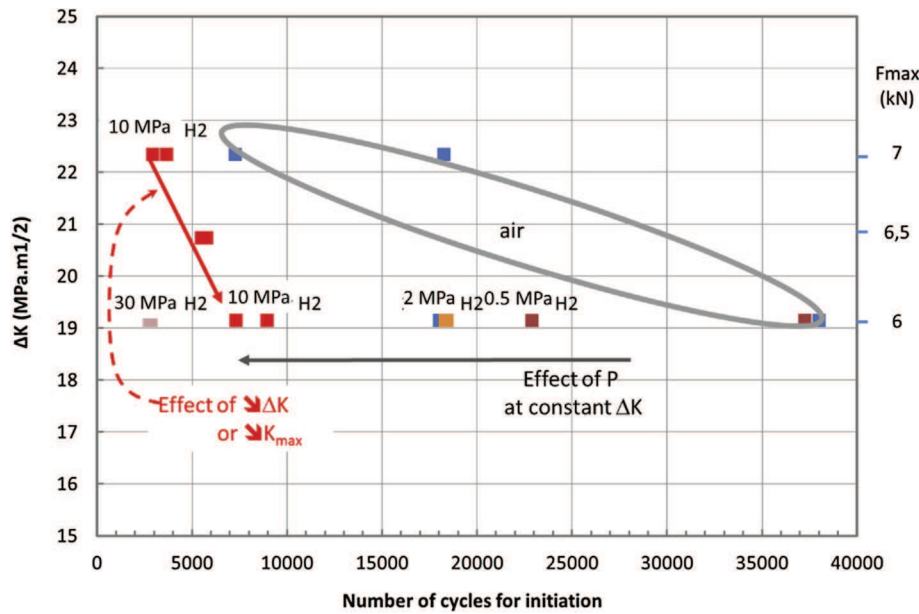
**Fig. 7 – Fatigue crack initiation results on SENT specimens (R = 0.1, RT).**

## Results and discussion

### Fatigue crack initiation

The fatigue crack initiation results obtained on the 25CrMo4 steel are presented in Fig. 7. In this figure, $\Delta K$ is calculated from elastic theory assuming the notch is a crack. All the specimens tested have the same geometry, thus the change in $\Delta K$ corresponds to a change of the applied load. All the tests presented here were performed at a load ratio R equal to 0.1. The applied load frequency was 0.5 Hz.

The first main results is that hydrogen gas has a strong influence on fatigue crack initiation. As it was expected, at 10 MPa $H_2$, a decrease of $\Delta K$ (or of $K_{max}$ since R is kept constant) leads to an increase of the number of cycles to initiation. However, the slope of the curve ($\Delta K$ versus $N_{init}$) under hydrogen is steeper than under air. These results seem to indicate that even if the plastic zone size is decreased the hydrogen affected zone remains sufficiently large to generate a defect with a critical size in terms of crack initiation.

The effect of pressure was studied for a given $\Delta K$ and R ratio. Tests performed under air or under $H_2$ pressure from 0.5 MPa up to 30 MPa are also displayed in Fig. 7 and in Fig. 8. First, the disparity in terms of number of cycle for initiation tends to be lower under hydrogen pressure than under air. Second, although these tests need to be confirmed by further

results, a continuous decrease of the number of cycles to initiation is observed as the pressure is increased. If confirmed, it would be necessary to check if this tendency continues up to 100 MPa. Indeed, such $H_2$ pressure is the working one in buffer pressure vessels in refueling station for example.

In Fig. 9, the topology of the crack initiation region is presented. In front of notch, up to approximately 500 μm from the notch tip, the fracture surface presents different steps with the height of ±100 μm. Such steps have also been identified under air.

A SEM analysis of the fracture surface in the crack initiation area is shown in Fig. 10 (low magnification) and in Fig. 11 (higher magnification). Under air or 0.5 MPa $H_2$, no main differences are observed. By contrast, the fracture surfaces obtained at $H_2$ pressures higher than 2 MPa reveal a clear change of morphology. Indeed, even in the first tens of μm in front of the notch tip, an intergranular appearance is frequently
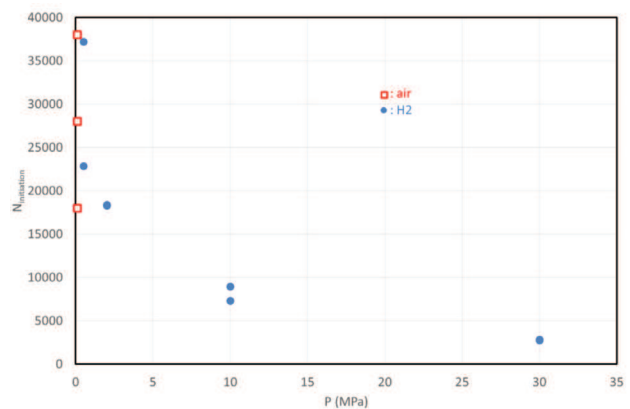


**Fig. 8 – Number of cycles for initiation versus pressure at F = 6 kN – R = 0.1.**
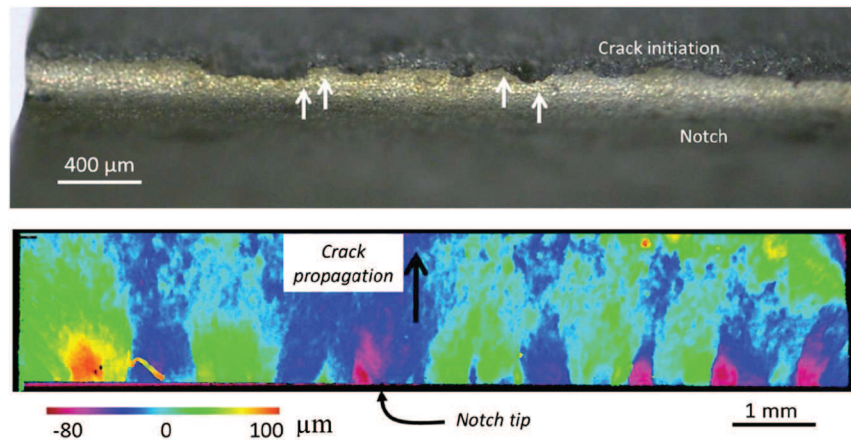
**Fig. 9 – Steps at crack initiation in front of the notch (10 MPa H$_2$, Fmax = 6 kN). The bottom figure displays the altitude perpendicular to the crack propagation, highlighting the presence of steps.**
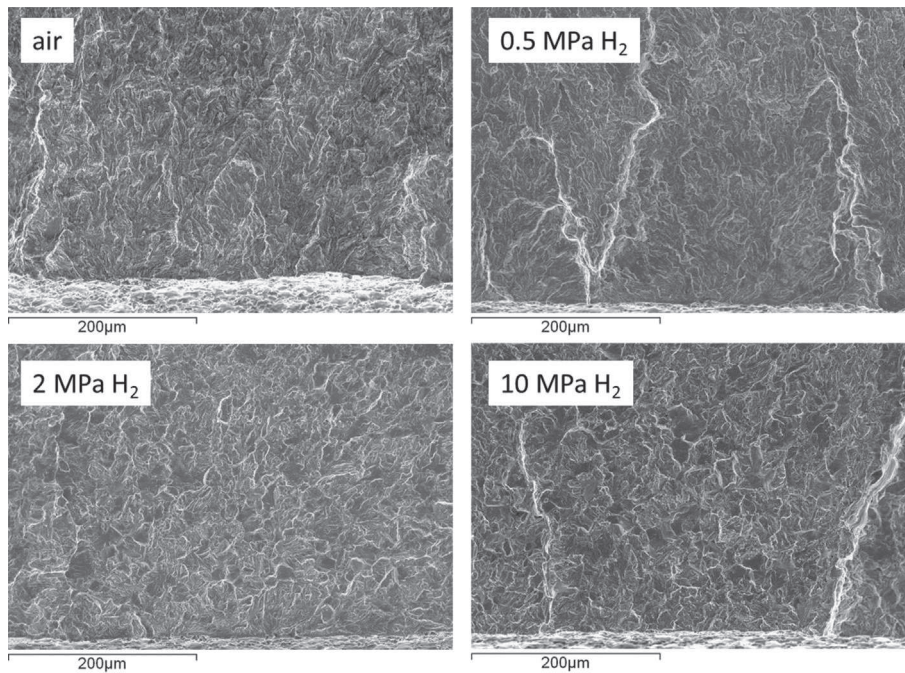


**Fig. 10 – Fracture surface in the initiation zone. Low magnification, the notch is on the bottom of all figures. In all cases, the loading is the same with F = 6 kN and R = 0.1. The notch tip is apparent at the bottom of each figure.**

observed, with also the presence of secondary cracks. The size of these zones is around 20 μm, which is in line with typical prior austenite grain size on low alloy Q&T steels. In parallel, EBSD analysis of the material microstructure in this region was carried out and the data were then treated with the ARPGE software [14,15]. This software allows to reconstruct the prior austenite parent grains from the orientation of the actual grains obtained after the Q&T heat treatment operation. From the first results of this running analysis, the prior austenite grains size was estimated close to 30 μm. Since no other microstructural elements have an equivalent size, one may reasonably state that the intergranular shape of H-assisted fracture is related to the prior austenite grains.

Few references deal with the influence of hydrogen on fatigue crack initiation. Studying 304 or 316L stainless steels, Murakami and Matsuoka [16] have shown that increasing the hydrogen concentration increased the number of cycles necessary for crack initiation to occur as compared to an uncharged specimen. By contrast, and for the same steels, other authors did not observe any influence of hydrogen on fatigue crack initiation [17]. Kesten developed a device to periodically increase the internal pressure of a tubular notched specimen on a quenched and tempered C–Mn steel [18]. The tests were performed under oil and hydrogen at 20 MPa. Results showed that the number of cycles for crack initiation drops by an order of magnitude when hydrogen is present.
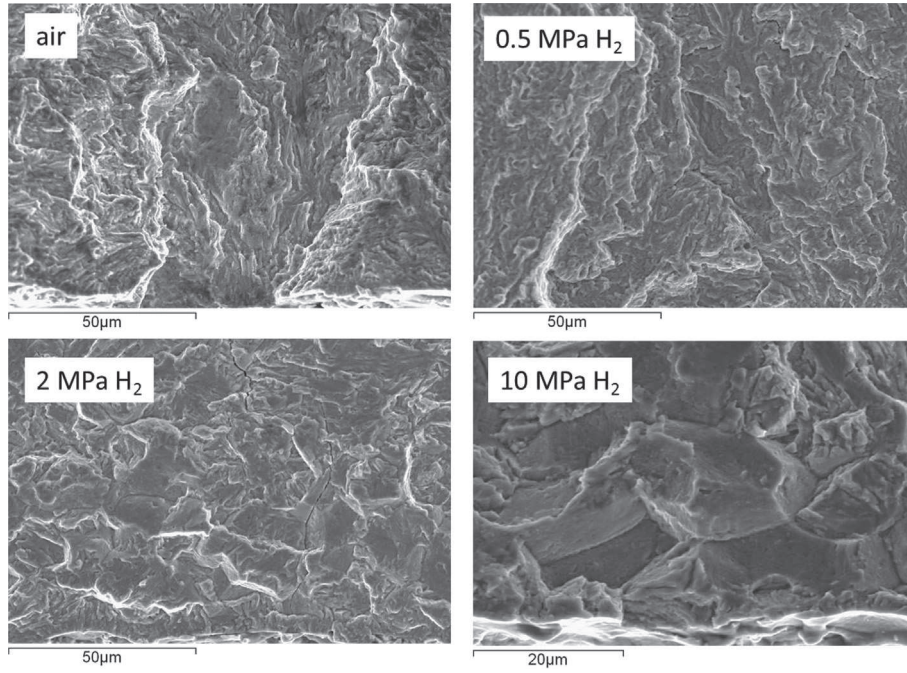
**Fig. 11** – **Fracture surface in the initiation zone. High magnification, the figures are all less than 100 μm from the notch tip. In all cases, the loading is the same with F = 6 kN and R = 0.1. The notch tip is apparent at the bottom of each figure.**

The comparison of the present results to the literature has to be done with care, as the crack initiation definition may not be the same. The observed changes of fracture morphology right from the first micrometers in the present study are a clear microstructural proof of the effect of hydrogen in the early stage of a crack. However, the present results may be explained by hydrogen enhanced fatigue or by no effect on crack initiation and a strong effect on small crack growth. To definitely clarify this point, a higher resolution measurement of crack length should be developed under hydrogen pressure, which remains quite challenging.

*Fatigue crack growth*

Although the hydrogen enhanced fatigue crack growth of CrMo steels has already been addressed by several authors [19–21], some points still remain to be clarified. In particular, it is recognized that the FCG rate under hydrogen should decrease to reach the value obtain under air when decreasing



**Fig. 12** – **Extrapolation of FCG data at low ΔK under H₂ pressure.**

ΔK, approaching the ΔK threshold (Fig. 12) [21,24]. However, the effect of the frequency and of the H₂ pressure at these low ΔK values are not well known, in particular due to the increasing duration of the tests under such loading conditions. However, extrapolating FCG rate values under hydrogen pressure from the classical ΔK range to low ΔK values may lead to a strong underestimation of the total life of a component as shown in Fig. 12.

Murakami [16] analyzed the effect of the testing frequency working on an SCM 435 CrMo steel on hydrogen precharged specimens. The authors observed that, above a given frequency depending on the initial hydrogen content in the specimen, the FCG rate under hydrogen tends to that obtained under air testing conditions. This change of behavior is linked to competition between the FCG rate and H diffusion rate leading to a critical FCG rate above which no effect of hydrogen can be observed. The diffusion length during one cycle is given by:

$$d = \sqrt{D/f} \qquad (2)$$

where f is the testing frequency (Hz) and D is the diffusion coefficient (m²/s). The crack increment during one cycle is obtained experimentally by the da/dn versus ΔK curves. Equaling these two lengths, one obtains an estimate of the frequency associated to this change of behavior (equation (3)) [25].

$$f = \dfrac{D}{\left[ \frac{da}{dn}(\Delta K) \right]^2} \qquad (3)$$

Dealing with CrMo steels, where the diffusion coefficient of hydrogen is still quite high, this critical FCG rate is relatively high. Although this should be experimentally proved by some
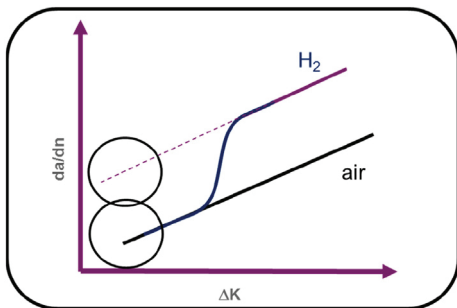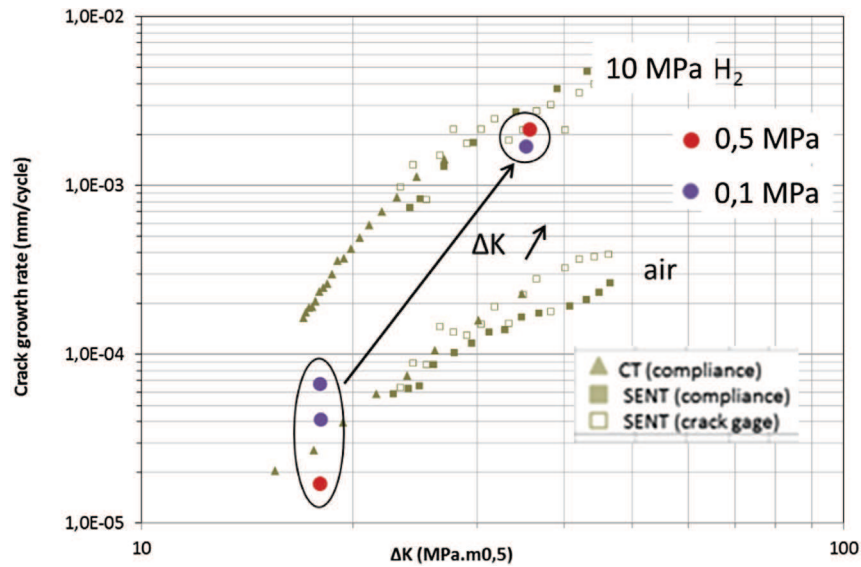
Fig. 13 — Fatigue crack growth on SENT specimens — Effect of low $H_2$ Pressure.

very long tests at very low frequency, one may expect no additional hydrogen effect on the FCG behavior when decreasing the frequency from [0.1–1] Hz range to lower frequencies more representative to the real component loading.

In Fig. 13, the data obtained during the present study on CT and SENT specimens under air and under several $H_2$ pressures are presented. First, these results confirm the statement performed in section 2.4: the FCG rates obtained by the compliance method and using the crack gages are equivalent. Thus, the use of crack gages is appropriate for both crack initiation and crack growth analysis when working under $H_2$ pressure. Second, the FCG rates obtained with both geometries are also equivalent. It has already been shown that for FCG there is no constrain effect, due to the small loading at the crack tip. This would not be the case for toughness measurements. Moreover, the crack propagation direction is not the same in SENT or CT specimens. In the SENT specimens the crack propagates through the thickness of the wall as for a real crack in the cylinder, whereas in the CT specimen, it propagates in the longitudinal (L) direction of the cylinder. The present results show that, in the case of the 25CrMo4 cylinders, there is no effect of the direction of crack propagation on the fatigue crack behavior.

The results obtained also show that the effect of $H_2$ pressure on the fatigue crack behavior is dependent on the loading. At low $\Delta K$ (14 MPa $m^{1/2}$) and pressures lower than 0.5 MPa, the FCG rate are roughly equivalent to that measured under air. Increasing $\Delta K$ leads to a change of behavior. Even at low pressure, the FCG rate is then found equivalent to that observed at high pressure. Performing tests at high $H_2$ pressure necessitates expensive dedicated devices. To identify a threshold pressure above which no additional $H_2$ pressure effects are observed would certainly be very convenient. The present results show that deriving such a threshold will not be straightforward. Another consequence of the coupled load-pressure dependence of the fatigue crack behavior, is that

the $\Delta K$ value where the behavior under hydrogen tends to reach the behavior under air is also certainly pressure dependent.

The fracture surfaces along the crack propagation path are displayed in Fig. 14. At a macroscopic scale, the fracture surfaces under hydrogen look flatter than under air. Under air, some fatigue striations perpendicular to the crack propagation direction are frequently observed. It is much harder to find them on the specimen tested under hydrogen at 10 MPa, their shape being however quite different. Another interesting feature is that intergranular areas are observed under hydrogen, as already observed on crack initiation zones. Here again, they have a size consistent with that of the prior austenitic grains.

At a lower magnification, some facets are observed. This has already been discussed by other authors on similar steels [11]. We also observed on the CrMo steel, that the surface proportion of these facets is higher under $H_2$ than under air at a given $\Delta K$.

## Conclusion

In this study, the fatigue cracking behavior obtained on a CrMo steel under hydrogen pressure have been presented. Both crack initiation and propagation have been addressed. In order to detect crack initiation, the use of crack gages under $H_2$ pressure has been validated. It has also been shown that these gages can be used to measure fatigue crack rate under $H_2$ pressure. The following main conclusions have been obtained.

First, the effect of $H_2$ pressure on crack initiation was analyzed. Defining crack initiation as a crack 0.1 mm long from the notch tip, the number of cycles to initiation was found to decrease with an increasing $H_2$ pressure from 0.5 MPa
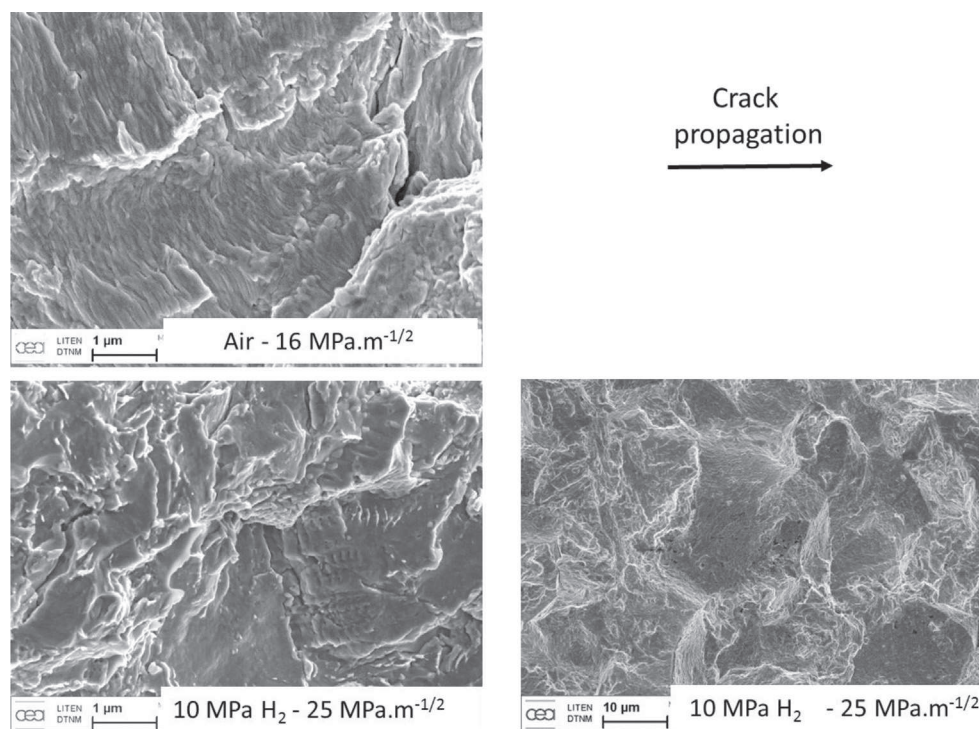
**Fig. 14 — Fracture surface during the FCG process.**

to 30 MPa. At this pressure, a reducing factor of 10 was observed.

Second, a coupled effect of $\Delta K$ and $H_2$ pressure has been evidenced on fatigue crack growth. Indeed, at low $\Delta K$ and low pressure (below 0.5 MPa $H_2$), no increase of the crack growth rate is observed whereas it is observed at 10 MPa $H_2$. By contrast, at higher $\Delta K$, the effect of $H_2$ at these low pressures is similar to that obtained at 10 MPa.

The analysis of the fracture surfaces shows that the crack paths in the initiation as well as in the propagation steps are affected by the prior austenitic grains.

However, the testing methodologies developed in the present paper are not able to quantitatively discriminate to discriminate between a real effect of hydrogen on fatigue crack initiation and an effect of hydrogen on the fast growth of small cracks.

Additional tests, including tests at higher pressures are foreseen within the MATHRYCE project to confirm these results. Moreover, numerical simulations are currently performed to analyze the results in terms of the local stress and strain fields including the plastic zone size and the level of hydrostatic stress.

## Acknowledgements

## REFERENCES

[1] Briottet L, Moro I, Escot M, Furtado J, Sallais D, Dey R, et al. Material testing and design recommendations for components exposed to hydrogen enhanced fatigue − the Mathryce project. Brussels: ICHS; 2013.

[2] Sims JR. Standards and codes to control hydrogen − induced cracking in pressure vessels and pipes for hydrogen gas storage and transport. In: Gangloff P, Somerday B, editors. Gaseous hydrogen embrittlement of materials in energy technologies1. Woodhead Publishing Limited; 2012.

[3] San Marchi C, Somerday B, Nibur K. Development of methods for evaluating hydrogen compatibility and suitability. Int. J. Hydrog Energy 2014;39:20434−9.

[4] Nanninga NE. Fatigue crack initiation and fatigue life of metals exposed to hydrogen. In: Gangloff P, Somerday B, editors. Gaseous hydrogen embrittlement of materials in energy technologies1. Woodhead Publishing Limited; 2012.

[5] ESIS P11-02. Technical recommendations for the extreme value analysis of data on large non-metallic inclusions in steels. Eur Struct Integr Soc 2002:29. ISSN 1616-2129.

[6] ASTM E2283-08. Standard practice for extreme value analysis of nonmetallic inclusions in steel and other microstructural features. 2008.

[7] ISO 11120-1999, Gas cylinders - Refillable seamless steel tubes for compressed gas transport, of water capacity between 150 l and 3000 l - Design construction and testing.

[8] Murakami Y. Metal fatigue: effects of small defects and nonmetallic inclusions. Elsevier; 2002.

[9] Trasatti S, Sivieri E, Mazza F. Susceptibility of a X80 to Hydrogen Embrittlement. Mater Corros 2005;56.

[10] Moro I, Briottet L, Lemoine P, Andrieu E, Blanc C, Odemer G. Hydrogen embrittlement susceptibility of a high strength steel X80. Mater Sci Engineering:A 2010;527(27−28):7252−60.

[11] Macadre A, Yano H, Matsuoka S, Furtado J. The effect of hydrogen on the fatigue life of Ni−Cr−Mo steel Envisaged for

Use as a storage Cylinder for a 70MPa hydrogen station. Int J Fatigue 2011;33(12):1608—19.

[12] Briottet L, Escot M, Moro I, Tamponi GM, Furtado J, Solin J, et al. Crack initiation and propagation under hydrogen-enhanced fatigue of a Cr-Mo steel for gaseous hydrogen storage. materials for hydrogen service. Anaheim, USA: ASME 2014 Pressure Vessels & Piping Conference; July 20-24 2014.

[13] Escot M, Briottet L, Moro I, Andrieu E, Blanc C, Odemer G, et al. Hydrogen-enhanced fatigue of a Cr-Mo steel for gaseous hydrogen storage. Gent, Belgium: Steel&Hydrogen 2nd Int. Conf. on Metals and Hydrogen; May 5-7 2014.

[14] Cayron C, Artaud B, Briottet L. Reconstruction of parent grains from EBSD data. Mater Charact 2006;57:386—401.

[15] Cayron C. ARPGE: a computer program to automatically reconstruct the parent grains from electron backscatter diffraction data. J Appl Cryst 2007;40:1183—8.

[16] Murakami Y, Matsuoka S. Effect of hydrogen on fatigue crack growth of metals. Eng Fract Mech 2010;77:1926—40.

[17] Gangloff R, Somerday B. Gaseous hydrogen embrittlement of materials in energy Technologies. Woodhead Publishing in Materials; 2012.

[18] Kesten M, Windgassen KF. Design of equipment to hydrogen fatigue service. Am Soc Metals, Metals Park OH 1982;44073:389—93.

[19] Macadre A, Artamonov M, Matsuoka S, Furtado J. Effects of hydrogen pressure and test frequency on fatigue crack growth properties of Ni—Cr—Mo steel candidate for a storage cylinder of a 70MPa hydrogen filling station. Eng Fract Mech 2011;78(18):3196—211.

[20] Matsuoka S, Tanaka H, Homma N, Murakami Y. Influence of hydrogen and frequency on fatigue crack growth behavior of Cr-Mo steel. Int J Fract 2010;168(1):101—12.

[21] Suresh. Fatigue of materials. Cambridge: Cambridge University Press; 1991.

[22] www.mathryce.eu.

[23] Somerday P, Sofronis P, Nibur KA, San Marchi C, Kirchheim R. Elucidating the variables affecting accelerated fatigue crack growth of steels in hydrogen gas with low oxygen concentrations. Acta Mater 2013;61:6153—70.

[24] Suresh S, Ritchie R. On the influence of environment on the load ratio dependence of fatigue thresholds in pressure vessel steels. Eng Fract Mech 1983;18:785—800.

[25] Moro I, Briottet L, Lemoine P, Doyen O, De Dinechin G. Fatigue crack growth of a C-Mn steel and associated weld under hydrogen pressure, 2012 International hydrogen conference. In: Hydrogen-materials interactions. Wyoming, USA: Jackson Lake Lodge; September 9-12, 2012.